Development of a CFD methodology for fuel-air mixing and combustion modeling of GDI Engines

T. Lucchini*, G. D'Errico*, L. Cornolti*, G. Montenegro*, A. Onorati*

**Politecnico di Milano, Dipartimento di Energia, Italy*

ABSTRACT

Simulation of GDI engines represents a very challenging task for CFD modeling. In particular, many sub-models are involved since the evolution of the fuel spray and liquid film formation should be modeled. Furthermore, it is necessary to account for both the influence of mixture and flow conditions close to the spark plug to correctly predict the flame propagation process. In this work, the authors developed a CFD methodology to study the air-fuel mixing and combustion processes in direct-injection, spark-ignition engines. A set of sub-models was developed to describe injection, atomization, breakup and wall impingement for sprays emerging from multi-hole atomizers. Furthermore, the complete evolution of the liquid fuel film was described by solving its mass, energy and momentum equations on the cylinder wall boundaries. To model combustion, the Extended Coherent Flamelet Model (ECFM) was used in combination with a Lagrangian ignition model, describing the evolution of the flame kernel and accounting for both for flow, mixture composition and properties of the electrical circuit. The proposed approach has been implemented into the Lib-ICE code, which is based on the OpenFOAM®technology. In this paper, examples of application are provided, including the simulation of the fuel-air mixing process in a real GDI engine and the prediction of the premixed turbulent combustion process in a constant-volume vessel for different operating conditions.

Introduction

In GDI engines, simulation of the full engine cycle is always necessary since in-cylinder charge motions, generated during the intake stroke, strongly influence the fuel-air mixing process and both turbulence levels and fuel distributions at spark-timing. To be applied to complex engine geometries, reliable mesh management algorithms are necessary, together with consolidated models to predict evolution of fuel spray and liquid film. To estimate the cylinder pressure evolution during combustion the flame kernel formation and growth processes should be described in detail, accounting for the local turbulence, flow and mixture fraction distributions in the region where the spark-plug is located.

In this work, a CFD methodology for full-cycle simulations of gasoline, direct-injection engines is presented. To this end, a set of specific modules was implemented by the authors inside the Lib-ICE code, which is a set of libraries and applications developed to simulate IC engines and based on the OpenFOAM®technology. Examples of application of Lib-ICE to engine simulations can be found in [1, 2, 3]. The presented simulation methodology is based on the use of multiple meshes to cover the entire simulation. To reduce the pre-processing time required for case set-up and case handling, suitable utilities were developed. The proposed approach for fuel-air mixing simulations accounts for the complete spray evolution (injection, break-up, evaporation, wall impingement) and also includes the liquid film dynamics. For what concerns the prediction of the combustion process, a new model, called *LaFKI* (Lagrangian Flame Kernel Ignition) has been recently developed by the authors. It describes the flame kernel formation and evolution by means of a set of lagrangian particles, convected by the mean flow and whose grow-rate is computed from both electrical circuit properties and local values of the laminar flame speed. During the ignition process, the flame surface density field is reconstructed from the distribution of the flame kernel particles, ensuring a very strict coupling between the Eulerian and Lagrangian phases.

This paper presents application and experimental of the proposed models, including gas exchange in an optical engine, fuel-air mixing in a GDI engine and spark-ignition combustion inside a constant-volume vessel during the flame kernel growth process.

*http://www.engines.polimi.it

Mesh management and simulation handling

The proposed approach for CFD simulation of IC engines is illustrated in Fig. 1. A multiple number of meshes is employed, so that each mesh is valid in a certain crank angle interval and during it the grid points are moved and the grid topology is eventually changed. Meshes should be created before running the calculations by commercial or open-source tools. The amount of required meshes mainly depends on combustion chamber geometry complexity and valve timing.

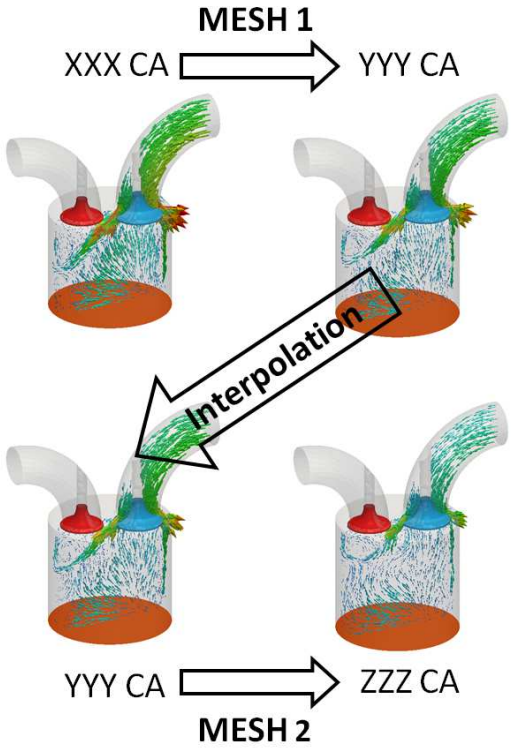

Figure 1: Summary of the strategy used for internal combustion engine simulation with moving meshes. Each mesh is used for a user-specified interval.

A cell-based, automatic mesh motion technique was applied to accommodate the motion of internal grid points according to the prescribed boundary motion [4, 5]. The Laplace equation is solved for the cell center displacement velocity field, $\mathbf{u}_c$, with constant or variable diffusivity γ and boundary conditions represented by the prescribed boundary motion. The grid points velocity field $\mathbf{u}_p$ is then extrapolated from $\mathbf{u}_c$ and used to compute the new point positions. To further preserve the mesh quality during motion it is also possible to use distance based diffusivity formulations or specify mesh-motion for an arbitrary number of points before solving the motion equation. Fig. 2 illustrates the proposed mesh setup when fully deforming meshes are used. The following regions can be distinguished:

1. fixed cells, in the intake and exhaust ports, together with zones in the cylinder where motion is not necessary (injector cavity, cells around the spark-plug),
2. cells moving with valve velocity. They can be usually found over the poppet of the valve,
3. deforming cells, whose motion is directly computed from Laplace equation.

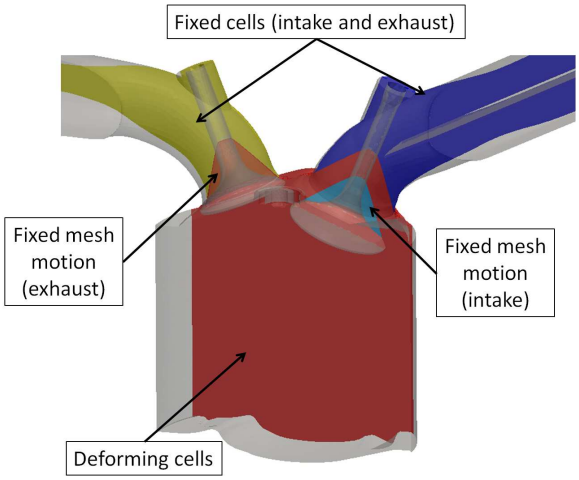

Figure 2: Mesh motion setup for fully deforming grids.

To reduce the pre-processing time that is required to import the different grids, create the required cases, run them and perform field mapping sequentially, a new set of utilities has been created in the context of this work:

- `engineCaseSetUp`: all the cases needed to perform the simulation are created automatically from a template one. Such utility imports automatically the meshes and decomposes the domain for parallel run.
- `runMultiCycleCase`: it sequentially runs the specified solver on each case and performs the field mapping operation on the next one. If needed, it also executes specific pre and post-processing utilities at run-time on each case.

All the information for case setup and simulation, such as validity interval of each mesh, required time-step, solver to be used and number of subdomains for parallel run are contained in a global file, called `engineControlDict`, that can be easily compiled by the users before running the two utilities. Fig. 3 provides additional details about how the two utilities handles pre-processing and simulation steps. For what concerns the solvers

used, they are fully compressible, support topological changes in the mesh and they are based on the so-called PIMPLE (PISO+SIMPLE) pressure-velocity coupling. Such algorithm allows higher time-steps and more stability, since the main transport equations (enthalpy, pressure, velocity) are under-relaxed at each time-step for each iteration except the last one. This ensure a smooth convergence of the results, like in the SIMPLE algorithm but with the same precision that is provided when PISO is used.

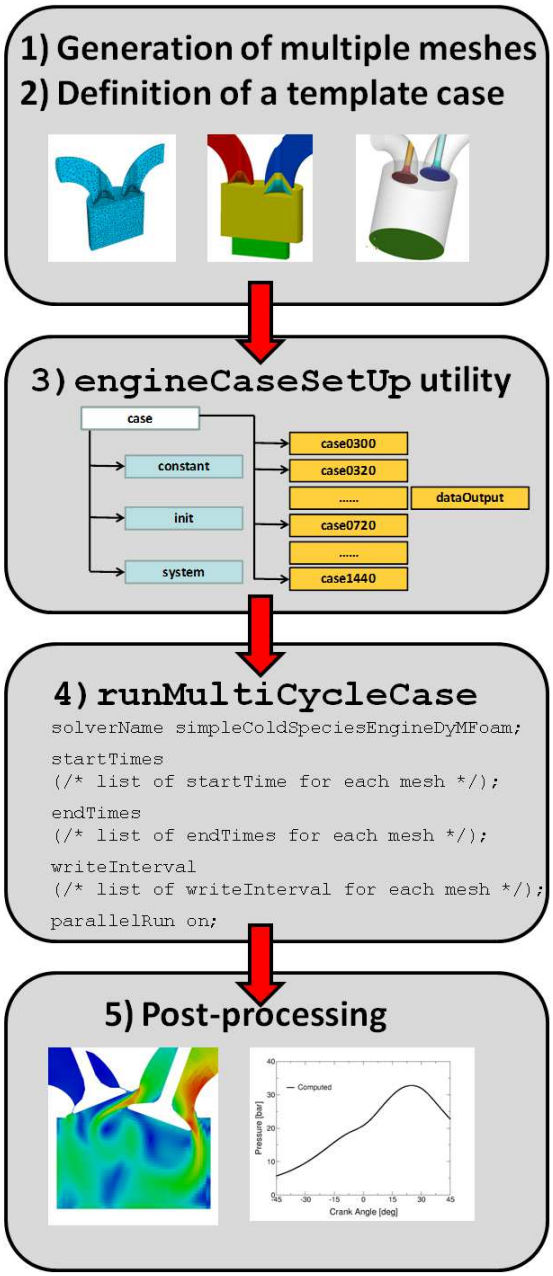

Figure 3: Full-cycle simulation strategy using LibICE.

The proposed approach has been extensively applied to simulate different engine geometries. This paper illustrates the simulation of the gas-exchange process under motored conditions in the SANDIA optical engine [6]. The engine has four valves per cylinder and a pent-roof combustion chamber. The low-tumble configuration was simulated, and a total number of three engine cycles was necessary to achieve results convergence. Details about the case set-up are illustrated in Table 1, while the mesh structure is shown in Fig. 4 where it is possible to see that it is mainly tetrahedral, despite in the valve region, where a hexahedral, flow-oriented structure was used. To simulate the full-cycle, a total number of 52 grids was used, each one valid for approximately 15 crank angle degrees. The mesh size ranges from 300 to 600 thousand cells and the standard k-ε model was used for turbulence.

Table 1: Geometry data of the SANDIA optical engine.

Bore × Stroke	85 × 92 mm
Compression ratio	11:1
IVO/IVC	346/-140 °CA
EVO/EVC	130/356 °CA
Engine speed	1500 rpm

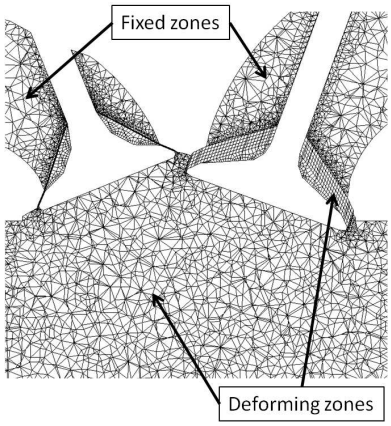

Figure 4: Mesh layout for the simulated optical engine.

Fig. 5 compares the computed and experimental in-cylinder pressure traces during the full cycle. Such result proves the validity of the proposed methodology for full cycle simulation in terms of mesh handling, initial and boundary conditions. Validation was then completed by comparing computed and experimental velocity fields at different crank angles during intake and compression strokes. Fig. 6(a) shows that the model correctly reproduces the experimental velocity field at IVC. It is possible to see the presence of two main streams originated from the valve sides and interacting on the piston surface. Furthermore, the location of the two vortexes that are created below

the valve by the incoming air jet is rather well captured. At the end of compression, see Fig. 6(b), the computed flow is almost aligned with the piston axis as also experimentally found.

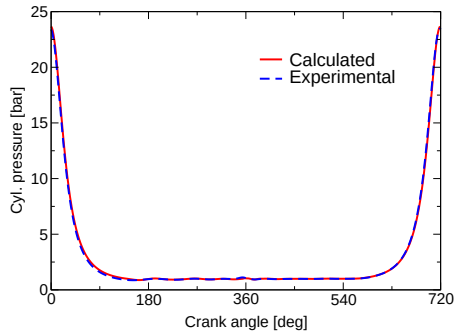

Figure 5: Comparison between computed and experimental cylinder pressure traces at motored conditions for the SANDIA optical engine.

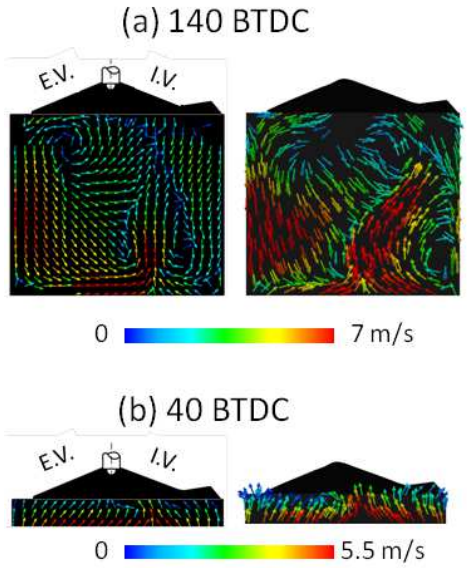

Figure 6: Comparison between experimental (left) and computed (right) velocity fields on the cylinder symmetry plane 140 and 40° before TDC.

Spray and liquid film models

The gasoline spray is described by the Lagrangian approach, and the liquid emerging from the nozzle is represented as a train of *blobs* whose diameter is progressively reduced by the growth of aerodynamic instabilities generated on the liquid jet surface. To account for the cavitation process that might usually take place inside GDI multihole atomizers, the initial diameter and velocities are estimated by the Nurick model, that correct their values by a computed area contraction coefficient. The initial spray angle is calculated by means of the Huh-Gosman model [7]. Droplet primary and secondary breakup are modeled by accounting for both Kelvin-Helmholtz and Rayleigh-Taylor instabilities [8]. Interaction between turbulence eddies and droplets was also handled while collision between droplets was neglected since it significantly increase the computational time.

In GDI engines, a good prediction of the liquid film generation and evolution is mandatory because it has a strong influence on the fuel-air mixing process. In the paper, to simulate the wall film a shallow water formulation was adopted for the flow equations, solving for mean thickness, momentum and energy in a conservative manner [9]. The liquid film equations were discretized on a curved 2-D surface in 3-D, accounting for its curvature and motion using the Finite Area Method. Faces of arbitrary shapes are supported, therefore it can be used with complex geometries like IC engines [1]. To account for the dynamics of the wall film on sharp surfaces (like valves), where new droplets are ejected, a liquid film atomization model was also included following the approach suggested by O'Rourke [10].

Simulations of gas exchange and fuel-air mixing were carried out for a turbocharged, GDI engine whose main data are illustrated in Tab. 2. The engine has variable valve timing on both the intake side, and a tumble flap that can be used to enhance air/fuel mixing.

Table 2: Main engine geometry data.

Displaced volume	1390 cm^3
Bore × Stroke	76.5 × 75.6 mm
Compression ratio	10:1
Valves per cylinder	4

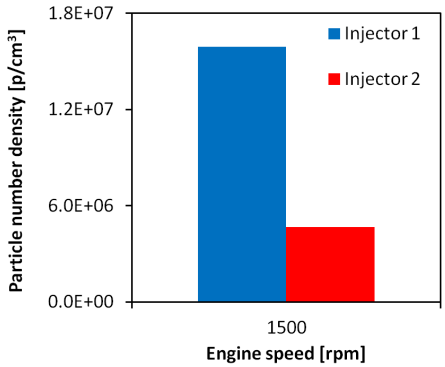

Figure 7: Effect of injector configurations on particulate emissions.

Two different configurations, with different spray patterns, were experimentally tested showing different levels of particle emissions, as illus-

trated in Fig.7. To understand such difference, CFD simulations were performed and computed results were analyzed in terms of:

- liquid film distribution on the cylinder walls
- air excess index distribution inside the cylinder
- evolution of the mixture inhomogeneity index during fuel injection and compression

In Fig. 8 it is possible to see that injector 1 deposits a higher amount of liquid film between the piston bowl and the cylinder liner. Such region, where a mixture very rich in fuel will be created, will be source of particulate emissions.

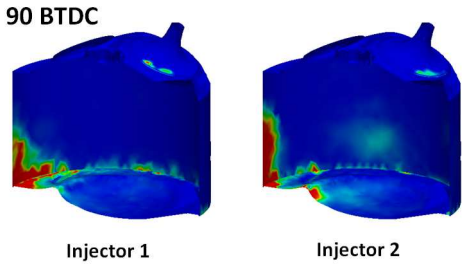

Figure 8: Distribution of liquid film during the compression stroke, 90 deg BTDC.

To better understand, on a quantitative point of view, the effects of the injector configuration on the fuel-air mixing process, a detailed investigation was performed in terms of mixture uniformity evolution and relative air/fuel ratio distribution at spark timing. Definition of uniformity index proposed by Lee et al. [11] was adopted:

$$H.I. = 1 - \frac{\sigma}{\sigma_{n,h}} \tag{1}$$

where σ represents the standard deviation of the fuel mass fraction, while $\sigma_{n,h}$ is defined as the standard deviation in a completely inhomogeneous condition where the fuel is not mixed with air at all:

$$\sigma_{n,h} = \sqrt{A/F}/\left(1 + A/F\right) \tag{2}$$

Fig. 9 shows that injector 2 produces a more homogeneous mixture and, as a consequence, the expected soot emissions will be lower.

Combustion model

In GDI engines, combustion is influenced by different phenomena such as electrical circuit properties, local flow conditions, turbulence intensity and fuel vapour distribution inside the combustion chamber. Within this context, the initial formation and evolution of the flame kernel need

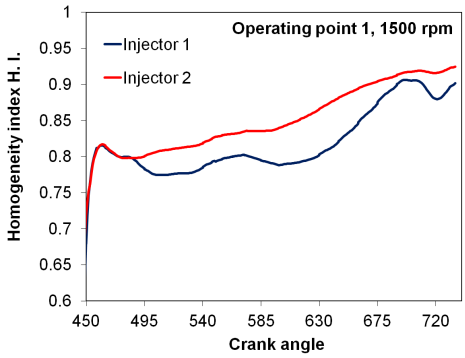

Figure 9: Distribution of liquid film during the compression stroke, 90 deg BTDC.

to be described in detail, since it will determine the subsequent turbulent flame propagation process and the cylinder pressure history. To predict the initial stage of spark-ignition combustion, a new model, called LaFKI (lagrangian flame kernel ignition) was developed by the authors. The model attempts to combine the most promising aspects of several approaches proposed in past works [12, 13, 14]. At spark timing, the spark-channel is represented by a set of lagrangian particles, that are placed along a line between the two electrodes. Particles are convected by the mean flow and, for all of them satisfying the ignition criterion, equations of mass and energy are solved. In these equations both the local laminar flame speed and the heat transferred from the electrical circuit through the spark electrodes are taken into account. After the particle tracking stage, the flame surface density distribution is reconstructed once particle positions and their radius is known. Such quantity is then used by the combustion model to calculate the fuel burning rate. The flame kernel model is de-activated once a turbulent flame structure is established. At that time, the Extended Coherent Flamelet Model [15] is used in the remainder of the simulation.

Fig. 10 illustrate a preliminary application of the proposed combustion model: a stoichiometric air/propane mixture (T = 300 K) is ignited at constant-pressure conditions (1 bar). The influence on the flame kernel growth of the velocity field in the vicinity of the spark-plug was evaluated for three different conditions: quiescent (0 m/s), moderate velocity (3.3 m/s), high velocity (7.4 m/s). Fig. 10(a) displays the predicted velocity field close to the spark-plug electrodes. In quiescent conditions, the flame kernel grows almost spherically, with a well defined region where burned gases can be found, as it can be seen from Figs. 10(b)-(c). The presence of a well-defined flow field in the spark region is responsible for two

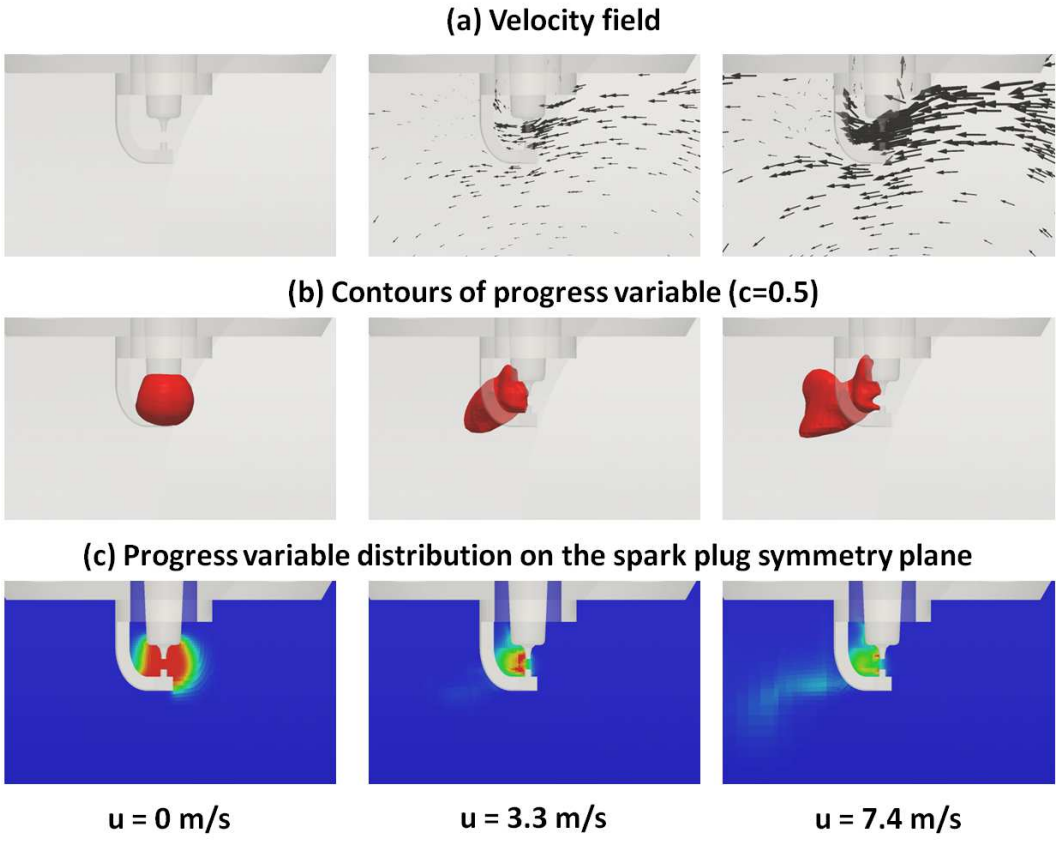

Figure 10: Computed flame kernel evolution for a stoichiometric air/propane mixture (p = 1 bar, T = 300 K) and three different ambient conditions: quiescent, moderate velocity (u = 3.3 m/s), high velocity (u = 7.4 m/s). (a): velocity field in the spark-plug region; (b): contours of progress variable equal to 0.5; (c): progress variable distribution on the spark-plug symmetry plane.

different phenomena, that are also experimentally observed:

- convection of the flame kernel by the flow and change of its shape,
- local turbulence might increases the flame speed if the flame kernel is well established,

Conclusions

This paper presented the set of models that have been recently implemented into the Lib-ICE code, based on the OpenFOAM technology, to handle simulation of gas-exchange, fuel-air mixing and combustion in gasoline, direct-injection engines. Selected examples of applications including gas-exchange in an optical engine, fuel-air mixing in a GDI engine, flame kernel growth at constant-pressure conditions, illustrate that the proposed CFD methodology is now completely consolidated and can be applied to the simulation of real engine configurations.

Acknowledgements

The authors would like to acknowledge Magneti Marelli Powertrain S.P.A. and Nissan Motor Company for funding the research activities related to CFD modeling of GDI engines.

References

[1] T. Lucchini et al., SAE Paper 2009-24-0015.

[2] T. Lucchini et al., SAE Paper 2011-24-0036.

[3] A. Montanaro et al. SAE Paper 2011-01-0685.

[4] T. Lucchini et al., COMODIA, 2008.

[5] T. Lucchini et al., SAE Paper 2007-01-0170.

[6] V.M. Salazar et al., SAE Paper 2009-01-2682.

[7] K. Y. Huh et al., Proc. of ICMF, 1991.

[8] R. D. Reitz., Atomization and Spray Technology, 1987.

[9] C. Bai et al., SAE Paper 960626.

[10] P.J. O'Rourke et al., SAE Paper 961961.

[11] J. Lee et al. SAE Paper 2000-01-1831.

[12] O. Colin et al., COMODIA, 2001.

[13] R. N. Dahms et al., Combustion and Flame, 2011.

[14] G. Bianchi et al., SAE Paper 2007-01-0146.

[15] T. Baritaud et al., Oil and Gas Science and Technology, 1999.